



## Effect of Annealing Temperature on the Structural Properties of $\text{Cu}_2\text{ZnSnS}_4$ Thin Films Prepared by Sol-Gel Method

Hassan J. Akbar<sup>1</sup>, Ali I. Salih<sup>2</sup> & Rafea A. Munef<sup>3</sup>

<sup>1</sup>Department of Physics, College of Sciences, Kirkuk University, Kirkuk, Iraq.

<sup>2</sup>Department of Physics, College of Education For Pure Sciences, Kirkuk University, Kirkuk, Iraq.

<sup>3</sup>Department of Physics, College of Sciences, Kirkuk University, Kirkuk, Iraq.

Received 5th November 2016, Accepted 1st December 2016

### Abstract

*Thin films of  $\text{Cu}_2\text{ZnSnS}_4$  (CZTS) have been successfully deposited on soda lime glass by spin coating technique. Raw material of sol-gel solution (precursors) consists of copper (II) acetate monohydrate, zinc (II) acetate dihydrate, tin (II) chloride dihydrate and Thiourea. CZTS thin films have been grown on clean soda-lime glass substrates at different annealing temperatures in the air for a period of 1 hour. The structural properties of these films have been studied by using X-ray diffraction XRD. The results of X-ray diffraction showed that all the CZTS films are polycrystalline (Hexagonal - Wurtzite) structure and preferred orientation along (100) to all sample, and the increasing annealing temperature led to an increase in the grain size, whereas dislocation density and micro strain decreases with the increase of annealing temperatures. The surface morphology of the thin films has been studied by using atomic force microscopes (AFM). The results of the atomic force microscope showed that the films grown by this technique have good crystalline and homogeneous surface. The Root Mean Square (RMS) and surface roughness values of thin films are decreased with increasing annealing temperature.*

**Keywords:**  $\text{Cu}_2\text{ZnSnS}_4$ , Thin films, Annealing Temperature, Sol-Gel method, Structural Properties.

© Copy Right, IJRRAS, 2016. All Rights Reserved.

### 1. Introduction

Energy demand is increasing following the development of industry, transportation and growth worldwide [1]. To meet the ever increasing demand for energy and to cope with the limited fossil resources available, photovoltaic solar energy production will become increasingly important. In order to reduce the cost of solar cells, new alternative materials in thin films have been investigated by researchers during recent

years for the development of next generation of efficient and cost-effective solar cells. Among them Copper Indium Gallium Diselenide (CIGS) and Cadmium Telluride (CdTe) have been successfully synthesized and have reached the commercialization stage [2,3]. However, the scarcity and toxicity of some elements such as Indium, Cadmium and Selenide could be a brake to the development of solar cells based on these materials. To develop new (PV) photovoltaic materials constituted of abundant elements in nature and which are cost-effective and eco-friendly is therefore an important and necessary issue to overcome the problem of limitation. The  $\text{Cu}_2\text{ZnSnS}_4$  (CZTS) material is one of the promising candidates to fulfill the above requirements. Because possesses huge potential for photovoltaic application due to its optimum energy band gap in the range (1.4-1.6) eV and high absorption coefficient ( $> 10^4 \text{ cm}^{-1}$ ) [4,5,6]. Several deposition techniques have been used for CZTS thin film manufacture, such as spray pyrolysis deposition [7], electron-beam-evaporation [8, 9, 10], rf magnetron sputtering deposition [11, 12], and sol gel deposition [13] and spin-coating deposition [14, 15,16]. However, Spin coating is currently the predominant technique employed to produce uniform thin films of photosensitive organic-inorganic materials with thickness of the order of micrometers and nano meters. The physics of spin coating can be effectively modeled by dividing the whole process into five stages which are (a) deposition, (b) spin-up, (c) spin-off and (d) evaporation of solvents (e) annealing. The first three are commonly sequential, but spin-off and evaporation usually overlap. Stage 3 (flow controlled) and stage 4 (evaporation controlled) are the two stages that have the most impact on final coating thickness. Spin coating has many advantages in coating operations with its biggest advantage being the absence of coupled process variables. Film thickness is easily changed by changing spin speed, or switching to a different viscosity photo resist. Another advantage of spin coating is the ability of the film to get progressively more uniform as it thins, and if the film ever becomes completely uniform during the coating process, it will remain so for the duration of the process. It is low cost and fast operating system [17]. In this work, the structural properties of CZTS thin films

### Correspondence

Hassan J. Akbar.

E-mail: hassanjalal457@gmail.com, Ph. +9647708907123

deposited by using sol-gel spin-coated deposition on clean soda-lime glass substrate at different annealing temperatures are presented.

## 2. Experimental Methods

CZTS precursor has been prepared by using : copper (II) acetate monohydrate (0.5 M), zinc (II) acetate dihydrate (0.25 M), tin (II) chloride dihydrate (0.25 M), thiourea (2 M), 2-methoxyethanol (50 mL) and diethanolamine (5 mL) were used. The solution of the precursors was dissolved in 2-metho and it was stirred at room temperature for 1 h to dissolve metal compounds completely. DEA was used as the stabilizer. After aging at room temperature in air for 24h, the prepared precursor solution was converted into sol-gel solution. The precursor sol solution was spin-coated onto SLG, which were previously cleaned into acetone, distilled water and ethanol at 3000 rpm for 30s followed by a solvent drying at 200 °C for 10 min on a hot plate. drying films were repeated 10 times to have a suitable thickness of the film. Finally, films were annealed at different temperatures (500, 550,600,650)°C using an electric furnace for 2 h in air. The X-ray diffraction patterns for the prepared films were obtained in a (Shimadzu XRD-6000) goniometer using copper target (1.5406 Å) and Atomic Force Microscopy (AFM) micrographs were recorded by using scanning probe microscope type (SPM- AA3000), Contact mode, supplied by Angstrom Advanced Inc.

## 3. Results and Discussion

### 3.1. X-Ray Diffraction

CZTS thin films deposited by sol-gel spin coating technique are examined by X-ray diffraction to find the structural characterization of the films. Figure. 1 shows the XRD patterns of the CZTS thin films obtained at different annealing temperature (500, 550,600, and650)°C. It can be noticed from the X-ray pattern all films have a polycrystalline structure with peaks identified at  $2\theta \sim 26^\circ, 28^\circ, 30^\circ, 33^\circ, 47^\circ$  and  $51^\circ$  positions corresponding respectively to the (100), (101), (102), (110) and (103) crystallographic directions of the hexagonal structure and matching well with those of the previously reported CZTS wurtzite structure [18].

Although there was no standard card for wurtzite CZTS in JCPDS databases, This structure can be obtained from the wurtzite ZnS by replacing Zn(II) with Cu(I), Zn(II) and Sn(IV) [19].

The strongest peak observed at Bragg's angle ( $2\theta = 26^\circ$ ) can be attributed to the (100) plane of the hexagonal CZTS, which is in agreement with other reports [20]. It can be noticed that  $2\theta$  position for (100) direction shifts to higher values as annealing temperature increases from 500 °C,550 °C to 600°C, whereas at annealing temperature of 650°C the  $2\theta$  shifts back to a lower value as shown in Table-1. The values of Full Width at Half Maximum (FWHM) of the peaks which decreases with annealing temperature.

The lattice constant was found to vary from  $a = 3.8968 \text{ \AA}$  to  $3.8738 \text{ \AA}$  and from  $c = 6.7495 \text{ \AA}$  to  $6.7096 \text{ \AA}$ . These values matching well with those of the previously reported CZTS wurtzite structure ( $a=3.8387 \text{ \AA}$ ,  $c=6.3388 \text{ \AA}$ ) [18]. It must be noted here that there are many peaks back secondary phases, which is unrelated to the CZTS phase. All these peaks were defined by (\*) in figure-1.

These secondary phases can be attributed to  $(\text{Cu}_2\text{S}, \text{Sn}_x\text{S}, \text{Sn}_2\text{S}_3, \text{CuS}_2)$  as reported by previous studies[21,22,23]. The possibility of the emergence of such secondary phases is the high proportion of thiourea, which lead to increase the S content, it can react with metal ions to form secondary Phases and as well the annealing environment here the air [24,25].

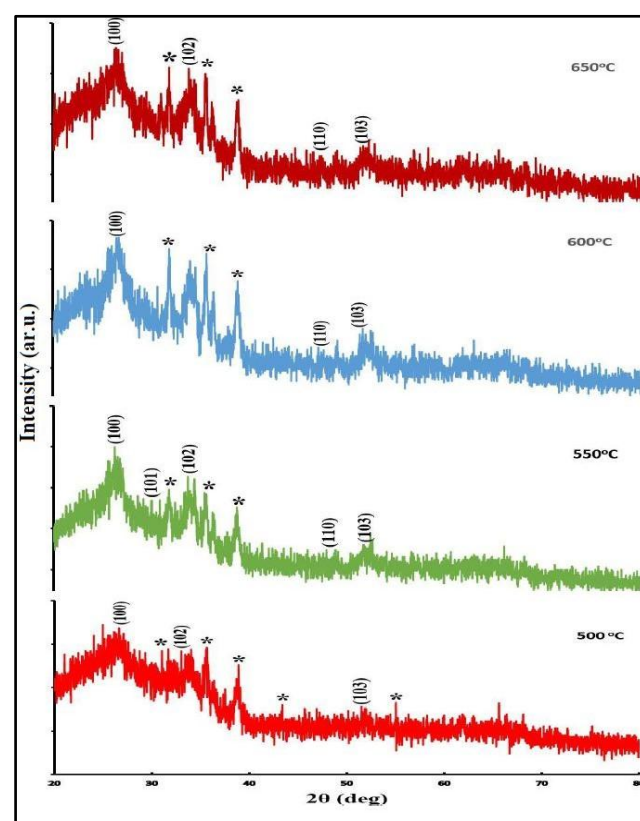


**Figure 1.** XRD pattern of CZTS thin films annealed at different temperatures.

The average grain size  $D$  of the films is calculated using Debye Scherrer's formula [26]:

$$D = K\lambda/\beta\cos\theta \dots\dots\dots(1)$$

Where  $K$  is the constant,  $\beta$  is the full width at half maximum (FWHM),  $\theta$  is the diffraction angle, and  $\lambda$  is wavelength of the X-ray, The  $K, \lambda$  values are taken as 0.9, 1.5406 Å for the calculations, respectively. The values of average grain size listed in Table-1 increase with the increase of annealing temperature for CZTS thin films as shown in Figure-2, this goes in agreement with previous studies which indicates the crystal structure improvement with annealing temperature [27].

**Table 1.** The structural parameters of CZTS thin films

Annealing temperature (A-T) (°C)	500 (°C)	550 (°C)	600 (°C)	650 (°C)
2θ (deg)	26.38 86	26.46 85	26.54 83	26.44 85
hkl	(100)	(100)	(100)	(100)
d (Å)	3.375	3.365	3.355	3.367
FWHM(deg)	1.96	1.52	1.38	1.84
D <sub>av</sub> (nm)	4.165	5.372	5.918	4.437
6×10 <sup>12</sup> (cm <sup>-2</sup> )	5.764	3.465	2.856	5.079
ε	0.008 3	0.006 5	0.005 9	0.007 8

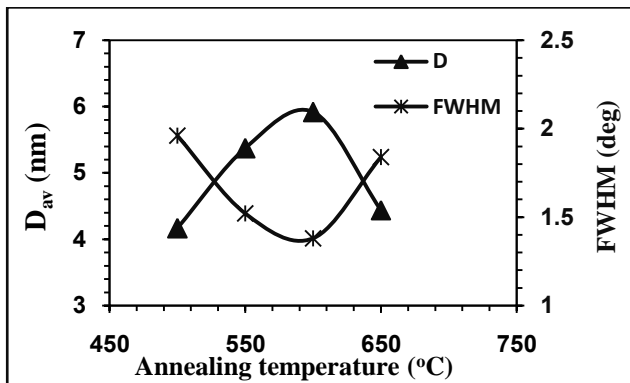


**Figure 2.** Grain size and full width of half maximum for CZTS thin films annealed at (500,550,600,650)°C.

The dislocation density  $\delta$  which represents the amount of defects in the film was determined from the formula [28]:

$$\delta = 1/D^2 \dots\dots\dots(2)$$

Where D is the grain size. It is observed that ( $\delta$ ) decrease with increasing annealing temperatures as shown in Table-1.

The micro strain is determined with the use of the following formula [29]:

$$\epsilon = \beta \cos\theta/4 \dots\dots\dots(3)$$

Where ( $\epsilon$ ) is the micro strain. It is observed that ( $\epsilon$ ) decrease with increasing annealing temperatures as shown in Table-1.

**3.2.AFM Results**

The Three-dimensional AFM images of Cu<sub>2</sub>ZnSnS<sub>4</sub> thin films are shown in Figure - 3. The size of the scanned area was (2µm×2µm). AFM images show that the films grown by this technique have good crystalline and homogeneous surface. The surface roughness and root mean square (RMS) for prepared thin films as shown in Table-2.

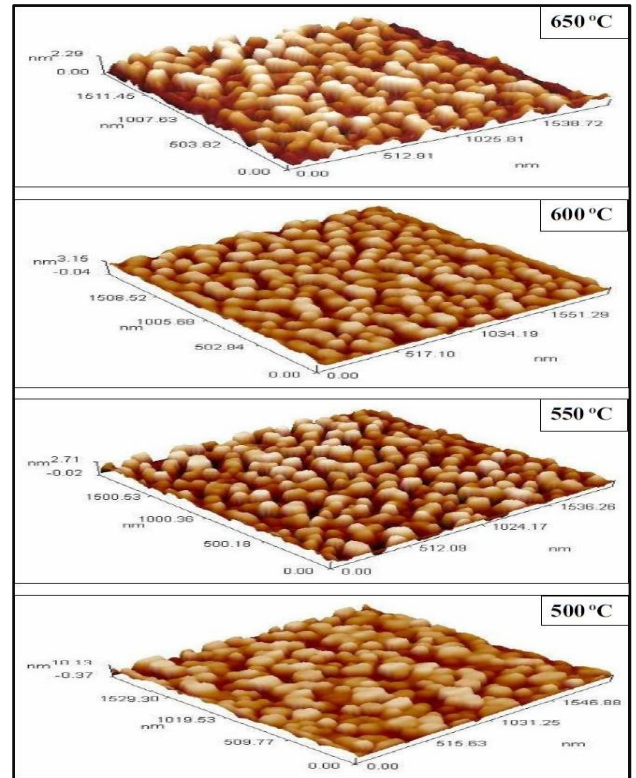


**Figure 3.** 3D AFM images of CZTS deposited films

**Table 2.** Surface roughness and root mean square of CZTS thin films.

A-T (°C)	Surface roughness (nm)	Root Mean Square (nm)
500	1.56	1.84
550	0.621	0.723
600	0.502	0.603
650	0.5	0.582

**Conclusions**

In the present paper, we have investigated CZTS thin films prepared on soda lime glass substrates by spin coating technique. XRD results reveal that the films are polycrystalline structure in Wurtzite phase and by orientation along (100) to all samples. The grain size increased with increasing annealing temperature, This leads to decrease in Full Width at Half Maximums (FWHM) of peak . It found there are many peaks back secondary phases, which is unrelated to the CZTS phase, These secondary phases attributed to (Cu<sub>2</sub>S, Sn<sub>x</sub>S, Sn<sub>2</sub>S<sub>3</sub>, Cu<sub>2</sub>S<sub>2</sub>). The possibility of the emergence of such secondary phases is due to the high proportion of thiourea, which lead to increase the S content, it can react with metal ions to form secondary Phases and also

the annealing environment here the air. AFM results showed that the values of the root mean square (RMS) and surface roughness of CZTS films decreased with the increase of annealing temperature.

### References

1. M. El Ouariachi, T. Mrabti, M. F. Yaden, Ka. Kassmi, B. Tidhaf, E. Chadli, F. Bagui and K. Kassmi, *J. Mater. Environ. Sci.* 2(S1) 538-543 (2011).
2. C.B. Murray, D.J. Norris, M.G. Bawendi, *Journal of the American Chemical Society*, 115 (19), pp 8706–8715(1993).
3. M. Jeon, T. Shimizu and S. Shingubara, *Materials Letters* 65.15: 2364-2367(2011).
4. Y. Cao, M. S. Denny Jr, J. V. Caspar, W.E. Farneth, Q. Guo, A. S. Ionkin, L. K. Johnson, M. Lu, I. Malajovich, D. Radu, H. D. Rosenfeld, K. R. Choudhury, and W. Wu, *Journal of The American Chemical Society*, Vol. **134**, 15644-15647 (2012).
5. N. Kamoun, H. Bouzouita, and B. Rezig, *Thin Solid Films*, 515, 5949-5952(2007).
6. X. Lin, J. Kavalakkatt, K. Kornhuber, S. Levchenko, M. C. Lux-Steiner and A. Ennaoui, *Thin Solid Films*, 535, 10-13(2013).
7. N. Kamoun, H. Bouzouita and B. Rezig, *Thin Solid Films* 515, p. 5949(2007).
8. H. Katagiri, N. Sasaguchi, S. Hando, S. Hoshino, J. Ohashi, and T. Yokotani, *Sol Energy Mater Sol Cells* 49, p. 407(1997).
9. H. Katagiri: *Thin Solid Films* 426, p. 480(2005).
10. H. Katagiri, K. Saitoh, T. Washio, H. Shinohara, T. Kurumadani and S. Miyajima, *Sol Energy Mater and Sol Cells* 65, p. 141(2001).
11. J. S. Seol, S. Y. Lee, J. C. Lee, H. D. Nam and K. H. Kim: *Sol Energy Mater and Sol Cells* 75, p.155(2003).
12. K. Jimbo, R. Kimura, T. Kamimura, S. Yamada, W. S. Maw, H. Araki, K. Oishi, and H. Katagiri: *Thin Solid Films* 515, p. 5997(2007).
13. K. Tanaka, N. Moritake, and H. Uchiki: *Sol Energy Matter Sol Cells* 91, p. 1199(2007).
14. W. Ki and H.W. Hillhouse, *Adv Energy Mater* 1: 732-735(2011).
15. T. K. Chaudhuri and D. Tiwari, *Sol Energy Mater Sol Cells* 101: 46-50(2012).
16. H. Park, Y. H. Hwang and B. S. Bae, *J Sol-Gel Sci Technol* 65: 23-27(2013).
17. N. Sahu, B. Parija and S. Panigrahi, *Indian Journal of Physics*, Vol. 83.493-502 (2009).
18. X. Lu, Z. Zhuang, Q. Peng, Y. Li, *Chem. Commun.* 47, 3141–3143 (2011).
19. J. H. N. Tchognia, Y. Arba, B. Hartiti, A. Ridah, J. M. Ndjaka and P. Thevenin, *Opt Quant Electron* 48:134 (2016).
20. J. H. N. Tchognia, Y. Arba, K. Dakhsi, B. Hartiti, J. M. Ndjaka, A. Ridah and P. Thevenin, *Opt Quant Electron* 48:255(2016).
21. H.C. Ni, C. H. Lin, K. Y. Lo, C. H. Tsai, T. P. Chen, J. L. Tsai and J. R. Gong, *ECS Journal of Solid State Science and Technology*, 4 (8) Q72-Q74 (2015).
22. N. Muhunthan, O. P. Singh, S. Singh and V. N. Singh, *International Journal of Photoenergy* Volume 2013, Article ID 752012(2013).
23. D. Seo, S. Lim, *J Mater Sci: Mater Electron*, 24 (10): 3756-3763,(2013).
24. Y. B. Kumar, P. U. Bhaskar, G. S. Babu & V. S. Raja. *physica status solidi (a)*, 207(1), 149-156, (2010).
25. J. H. Nkuissi Tchognia, Y. Arba, B. Hartiti, K. Dakhsi, J. M. Ndjaka, A. Ridah, P. Thevenin, *J. Mater. Environ. Sci.* 6 (8) 2120-2124(2015).
26. Y. B. Kumar, G. S. Babu, P. U. Bhaskar and V. S. Raja, *Solar Energy Materials and Solar Cells*, 93(8), 1230-1237(2009).
27. S. Kahraman, S. Çetinkaya, M. Podlogar, S. Bernik, H. A. Çetinkara and H. S. Güder, *Ceramics International* 39, 9285–9292(2013).
28. J. Henry, K. Mohanraj and G. Sivakumar, *Journal of Asian Ceramic Societies*, 4(1), 81-84, (2016).
29. P. Kathirvel, D. Manoharan, S. M. Mohan and S. Kumar, *J Optoelectron Biomed Mater*, 1, 25-33, (2009).